Sci. Annals, Fac. Phys. & Mathem., Univ. Thessaloniki, 16. 281 (1976)

COMPUTED PROFILES OF EDGE DISLOCATION IMAGES LYING CLOSE TO THE CRYSTAL SURFACE

by

J. G. ANTONOPOULOS

(Physics Department, University of Thessaloniki)

(Introduced by Prof. N. A. Economou)

(Receivel 25.10.76)

Abstract. *Computed profiles of edge dislocation images are given. Surfaee relaxation and stacking-fault displacements were taken into account in constructing the programme. Results show that it is, under certain eonditions, possible to distinguish among a Shockley partial, a Frank partial and a perfect dislocation.*

1. INTRODUCTION

The equations which describe the dynamical theory of electron diffraction contain a term for the displacement field around a defect. The form of this term for a dislocation, derived on the basis of linear isotropic elasticity theory, depends on the products $\mathbf{g}\cdot\mathbf{b}$ and $\mathbf{g}\cdot\mathbf{b}\times\mathbf{u}$ (where $\mathbf{g}$ is the diffracting vector, $\mathbf{b}$ the Burgers vector and $\mathbf{u}$ a unit vector along the dislocation line), in such a way that if a value of $\mathbf{g}$ making these factors zero can be found the whole displacement term is zero and the dislocation is invisible[1,2,3]. These two products are known as the «invisibility criteria» and for most cases are sufficient to identify a dislocation. In the cases where this is not so, computer calculations are needed[3,4]. There are two methods of identifying defects by computing. The most common method is to do intensity profiles in which a graph of the electron intensity as a function of the position along a line perpendicular to the dislocation is constructed. The second method is to form a complete two-dimensional image, that is to make a theoretical micrograph using the calculated intensities.

The appearance of a defect lying close to one of the surfaces of the crystal is affected by the so-called surface relaxation effect, and the invisibility criteria do not always hold[5]. The aim of this paper is to present computed intensity profiles for edge dislocations which lie very close to the surface and are parallel to it. When the dislocation

is a partial one, the existence of stacking fault is taken into account. The results were obtained using a new subroutine for the displacement field for a usual otherwise intensity-computing programme and indicated that a distinction among a Shockley partial, a Frank partial and a perfect dislocation shound be possible.

2. THEORY.

The general equations describing the state of stress at a point of an elastic medium are[6,7,8]

$$\begin{aligned}
\sigma_{xx} &= c_{11}\varepsilon_{xx} + c_{12}\varepsilon_{yy} + c_{13}\varepsilon_{zz} + c_{14}\varepsilon_{yz} + c_{15}\varepsilon_{zx} + c_{16}\varepsilon_{xy} \\
\sigma_{yy} &= c_{21}\varepsilon_{xx} + c_{22}\varepsilon_{yy} + c_{23}\varepsilon_{zz} + c_{24}\varepsilon_{yz} + c_{25}\varepsilon_{zx} + c_{26}\varepsilon_{xy} \\
\sigma_{zz} &= c_{31}\varepsilon_{xx} + c_{32}\varepsilon_{yy} + c_{33}\varepsilon_{zz} + c_{34}\varepsilon_{yz} + c_{35}\varepsilon_{zx} + c_{36}\varepsilon_{xy} \\
\sigma_{yz} &= c_{41}\varepsilon_{xx} + c_{42}\varepsilon_{yy} + c_{43}\varepsilon_{zz} + c_{44}\varepsilon_{yz} + c_{45}\varepsilon_{zx} + c_{46}\varepsilon_{xy} \\
\sigma_{zx} &= c_{51}\varepsilon_{xx} + c_{52}\varepsilon_{yy} + c_{53}\varepsilon_{zz} + c_{54}\varepsilon_{yz} + c_{55}\varepsilon_{zx} + c_{56}\varepsilon_{xy} \\
\sigma_{xy} &= c_{61}\varepsilon_{xx} + c_{62}\varepsilon_{yy} + c_{63}\varepsilon_{zz} + c_{64}\varepsilon_{yz} + c_{65}\varepsilon_{zx} + c_{66}\varepsilon_{xy}
\end{aligned} \tag{1}$$

The strains ε are given by

$$\varepsilon_{xx} = \frac{\partial U_x}{\partial x} \quad , \quad \varepsilon_{yy} = \frac{\partial U_y}{\partial y} \quad , \quad \varepsilon_{zz} = \frac{\partial U_z}{\partial z}$$

$$\varepsilon_{xy} = \frac{\partial U_x}{\partial y} + \frac{\partial U_y}{\partial x} \, , \; \varepsilon_{zx} = \frac{\partial U_z}{\partial x} + \frac{\partial U_x}{\partial z} \, , \; \varepsilon_{yz} = \frac{\partial U_y}{\partial z} + \frac{\partial U_z}{\partial y} \tag{2}$$

where U_x, U_y, U_z are the displacements along the x,y,z axes. There are 36 elastic constants c_{ij} (i, j=1,2,...,6). In an isotropic f.c.c. material these are reduced to only two, the Lame's constants λ and μ, and equations (1) become

$$\begin{aligned}
\sigma_{xx} &= (\lambda + 2\mu)\varepsilon_{xx} + \lambda\varepsilon_{yy} + \lambda\varepsilon_{zz} \\
\sigma_{yy} &= \lambda\varepsilon_{xx} + (\lambda + 2\mu)\varepsilon_{yy} + \lambda\varepsilon_{zz} \\
\sigma_{zz} &= \lambda\varepsilon_{xx} + \lambda\varepsilon_{yy} + (\lambda + 2\mu)\varepsilon_{zz} \\
\sigma_{yz} &= \mu\varepsilon_{yz} \\
\sigma_{zx} &= \mu\varepsilon_{zx} \\
\sigma_{zy} &= \mu\varepsilon_{xy}
\end{aligned} \tag{3}$$

If the plane x, y at z=0 is a free surface, then the conditions

$$\begin{aligned} &\sigma_{zz} = 0 && \text{for } z < 0 \\ \text{and} \quad &\sigma_{zz} = \sigma_{zx} = \sigma_{zy} = 0 && \text{at } z = 0 \end{aligned} \tag{4}$$

should be satisfied. These are the conditions for complete surface relaxation.

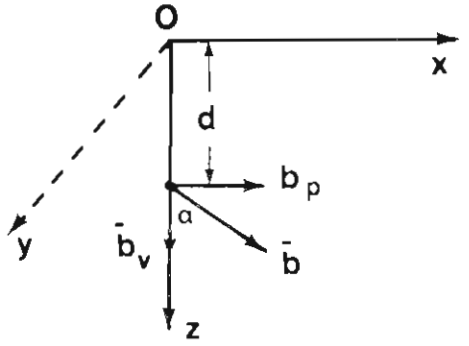

Fig. 1.

Suppose that a dislocation parallel to the y axis and with Burgers vector at an arbitrary angle α with the z axis lies at a distance d from the free surface (Fig. 1). To satisfy the conditions (4) an image dislocation with opposite Burgers vector is introduced at the image point $z = -d$. To simplify the problem the original dislocation is resolved into two component dislocations: one with Burgers vector $b_v = b\cos\alpha$, parallel to the z axis, and the other with Burgers vector $b_p = b\sin\alpha$, parallel to the x axis. Then each component dislocation is treated separately and the total stress field is obtained by suitable superposition of the two solutions. Head[9] has solved this problem for the case of edge dislocations. Using his equations for the stress field, the following component displacements were derived

$$U_{Lv} = \frac{b_v}{4\pi(1-\nu)}\left\{2(1-\nu)\left[\tan^{-1}\left(\frac{x}{z-d}\right) - \tan^{-1}\left(\frac{x}{z+d}\right)\right] + \frac{(z-d)x}{(z-d)^2+x^2}\right.$$

$$\left. - \frac{x\,[z+(3-4\nu)d]}{(z+d)^2+x^2} - \frac{4dzx(z+d)}{[(z+d)^2+x^2]^2}\right\}$$

$$U_{x_v} = \frac{b_v}{4\pi(1-\nu)}\left\{\frac{1-2\nu}{2}\log\frac{(z+d)^2+x^2}{(z-d)^2+x^2} - \frac{(3-4\nu)d(z+d)}{(z+d)^2+x^2} - \frac{(z-d)^2}{(z-d)^2+x^2} + \frac{z(z+3d)}{(z+d)^2+x^2} - \frac{4dzx^2}{[(d+z)^2+x^2]^2}\right\}$$

$$U_{z_p} = \frac{b_p}{4\pi(1-\nu)}\left\{\frac{1-2\nu}{2}\log\frac{(z-d)^2+x^2}{(z+d)^2+x^2} - \frac{(z-d)^2}{(z-d)^2+x^2} + \frac{z(z-d)}{(z+d)^2+x^2} - \frac{(3-4\nu)d(z+d)}{(z+d)^2+x^2} + \frac{4dzx^2}{[(z+d)^2+x^2]^2}\right\}$$

$$U_{x_p} = \frac{b_p}{4\pi(1-\nu)}\left\{-2(1-\nu)\left[\tan^{-1}\left(\frac{z-d}{x}\right) - \tan^{-1}\left(\frac{z+d}{x}\right)\right] - \frac{(z-d)x}{(z-d)^2+x^2} + \frac{(3-4\nu)dx}{(z+d)^2+x^2} + \frac{zx}{(z+d)^2+x^2} - \frac{4dxz(z+d)}{[(z+d)^2+x^2]^2}\right\}$$

where ν is Poisson's ratio. Therefore, the total displacements are

$$\begin{aligned} U_x &= U_{x_v} + U_{x_p} \\ U_z &= U_{z_v} + U_{z_p} \end{aligned} \qquad (5)$$

Equations (5) formed the basis of the subroutine used to calculate the displacements.

3. CONSTRUCTION OF THE PROGRAMME.

The programme makes use of the equations of the dynamical theory of image contrast[1]. The main programme enables calculations to be carried out both with or without the collumn approximation[10], using up to four beams.

The subroutine DISP, which has been constructed for the displacement field, is based on equations[5]. Then the stacking fault of the partial dislocations is taken into account. This is done not by introducing a phase factor in the Fourier transform for the crystal potential in the main programme, but by removing (in DISP) a vertical dis-

continuity and placing it on the stacking fault plane. This last operation is achieved by adding or substracting the corresponding dislocation Burgers vector. The relevant part of the programme is shown in Appendix A.

The DISP is written in such a way that profiles of five possible edge dislocations are printed out in one run of the programme, saving computing time. The geometry of the co-ordination system used and the five Burgers vectors are shown in Fig. 2. There is only one perfect

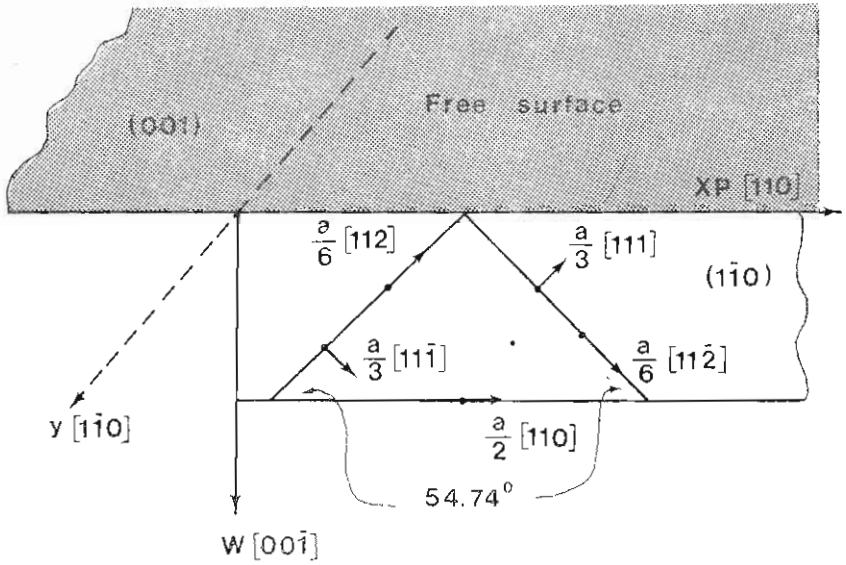

Fig. 2. The coordination system used to construct the DISP subroutine. Also shown are the Burgers vector of the five possible edge dislocations with their lines along [1$\bar{1}$0] direction

dislocation among them, the one with Burgers vector $a/2$ [110.] To distinguish each dislocation two parameters are used; the integral variable MD=1, 2,..., 5 and the angle A between the vectors w and b. Fig. 3 illustrates the five cases. The faulted regions, where a Burgers vector is added or substracted to the displacement field, are shown as shaded areas. A simplified axes transformation is employed, which allows rotation of the only specimen around the y axis, that is around the dislocation line itself. Rotation around any arbitrary axis would make the transformation very complex.

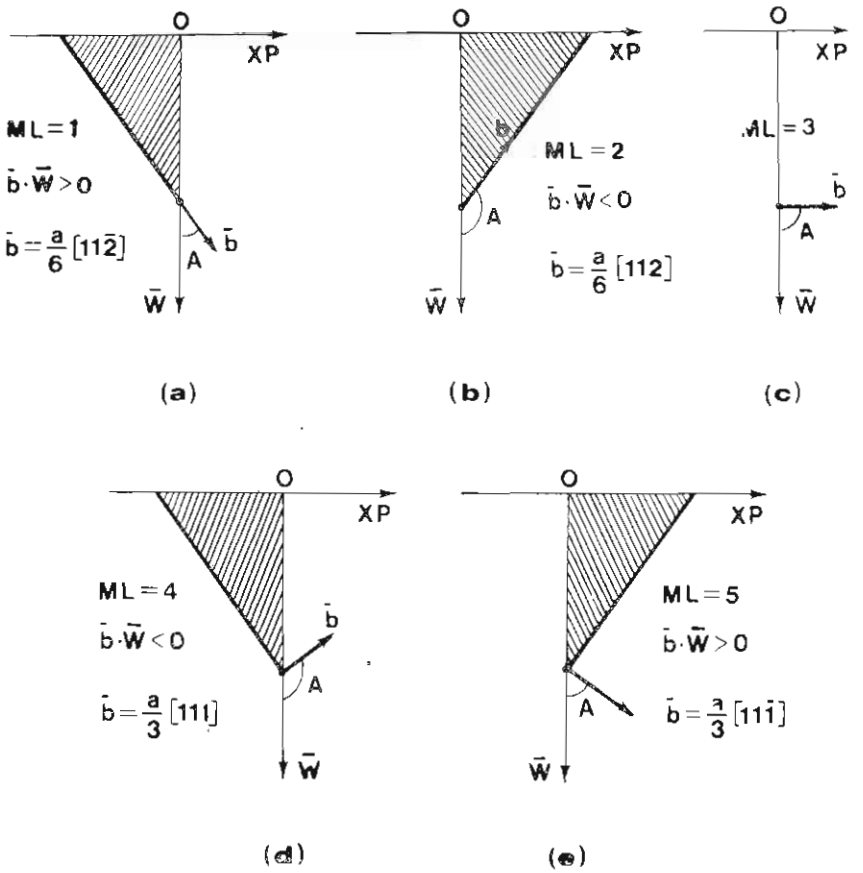

Fig. 3. The five considered dislocations, each shown separately. Thick lines represent the stacking fault planes. The plane of the paper is the (1$\bar{1}$0) and the dislocation lines are coming out of the paper. Parameters ML and A are also shown.

4. RESULTS AND DISCUSSION

The UNIVAC 1106 computer of the University of Thessaloniki was used to carry out computations. The programme was applied to a theoretical situation where the dislocations are situated in different depths from the surface of a copper single crystal. The anomalous absorption parameters and Smith-Burge's constants were taken from the literature[11-12], and the column approximation was always used. Most of the profiles were calculated for the weak-beam case[13], in which the diffra-

ction spot 3g is strongly excited and the spot g is used to form the image.

Figure 4 shows computed profiles of bright field images for dislocations well below the free surface (Fig. 4a) anf close to it (Fig. 4b). Computations were carried out using two beams, with g = 220 stron-

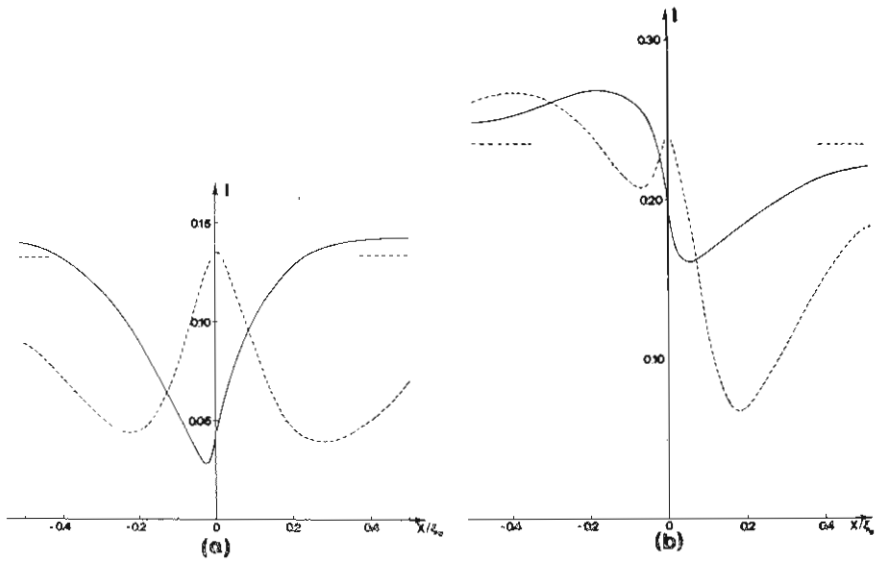

Fig. 4. Computed bright-field profiles of a Shockley partial (solid lines, g.b=*2/3) and a perfect dislocation (broken lines,* g.b=*2) with g=[220] strongly excited and* w_g *=0. Dislocations are situated at a depth of 1.3*ξ_g *in a foil 3.0*ξ_g *thick in (a) and at a depth of 0.06*ξ_g *in a foil 2.0*ξ_g *thick in (b).* (ξ_g = 419 Å).

gly excited ($w_{220} = 0$), and ignoring the stacking fault. In Fig. 4a the dislocations are at a depth of 1.3 ξ_g in a foil 3.0 ξ_g thick. The Shockley partial (**g**·**b**=2/3) appears as a dark line, whereas the perfect dislocation (**g**·**b**=2) appears as two dark lines in accordance with the theory[1]. In Fig. 4b the dislocations are at a depth of 0.06 ξ_g in a foil 2.0 ξ_g thick. The profiles here are significantly different from those in Fig. 4a, showing pronounced black-white contrast, due to the surface relaxation effect. This result agrees with other computed images[5,15].

In Fig. 5 the effect of the stacking fault is shown. The profiles are for a weak-beam situation when the dislocations are at a depth of 0.25 ξ_g in a foil 2.0 ξ_g thick, and with $w_{000} = +1$. Fig. 5a is a profile of the Shockley partial with $b = a/6$ [112] (see fig. 2b) and Fig. 5b of the

Frank partial with b=α/3 [111] (see fig. 2d). Broken lines are the dislocation profiles when the stacking fault is not taken into account. The difference in the profiles and the appearance of fringes in the regions where the stacking fault is considered are obvious.

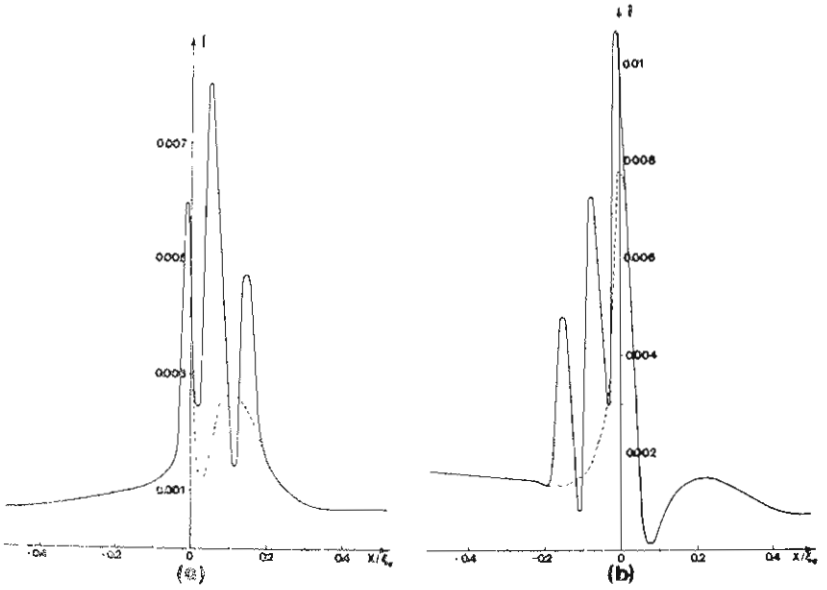

Fig. 5. The effect of the introduction of a stacking fault discontinuity (solid lines) on the original profile of the dislocation (broken lines). Profiles are for weak beam images of dislocations at a depth 0.25 ξ_g in a foil 2.0ξ_g thick. g=[220] and $w_{3g} = +1$. a) $\frac{a}{6}$ [112] Shockley partial b) $\frac{a}{3}$ [111] Frank partial.

In Fig. 6 the five dislocations are situated at a depth of 0.06 ξ_g in a crystal 2.0 ξ_g thick. Profiles are for the weak reflection g = [220] with $w_{3g} = +1.0$. It is clear that a) The intensity of the Shockley dislocation $\alpha/6$ [112] is about three times higher than the intensity of the other Shockley dislocation $\alpha/6$ [11$\bar{2}$], bnt it is about one half of the intensity of the perfect dislocation $\alpha/2$ [110]. b) The intensity of the Frank dislocation $\alpha/3$ [111], is about two times higher than the intensity of the other Frank dislocation $\alpha/3$ [11$\bar{1}$], but almost the same compared to the intensity of the perfect dislocation $\alpha/2$ [110]. These differences could be used as a criterion to distinguish a Shockley partial from a Frank partial, when a perfect dislocation is also present. The perfect dislocation could be traced using two opposite reflections as shown in

Fig. 7, where profiles of the dislocations $\alpha/2[110]$, $\alpha/3[111]$ and $\alpha/6[112]$ in the weak reflection g $=[220]$ are plotted, the other conditions being as in Fig. 6. Comparing the profiles of Figures 6 and 7, it is clear that by changing from $+g$ to $-g$ the image of the perfect dislocation simply

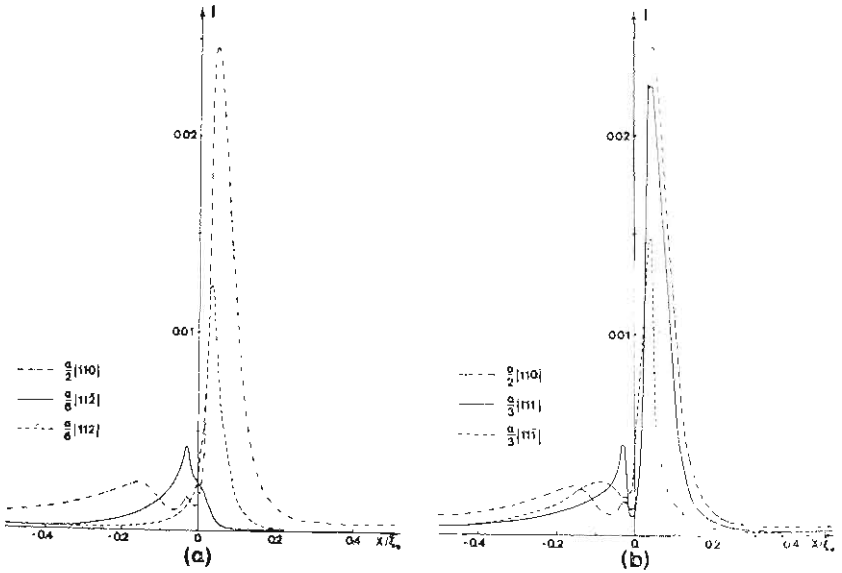

Fig. 6. Weak-beam image profiles for dislocations at a depth $0.06\xi_g$ in a foil $2.0\xi_g$ thick. g $=[220]$ and $w_{3g} = +1$.

changes position relatively to the real position of the dislocation (at x $=0$), the intensity remaining unchanged. In the case of partial dislocations the images change not only position but also intensities; the Shockley $\alpha/6[112]$, which is strong in Fig. 6a, becomes weak in Fig. 7 and the Frank $\alpha/3[11\bar{1}]$, which is weak in Fig. 6b, becomes strong in Fig. 7. This could then be taken as a criterion for dinstinguishing a perfect from a partial dislocation.

Finally, Fig. 8 is a computed bright field profile for a Shockley partial dislocation with $b=\alpha/6[\bar{1}1\bar{2}]$, lying parallel to the (001) foil surface, along the [110] direction at a depth of 0.103 ξ_g in a crystal 4.2 ξ_g thick. The diffraction vector is g$=[111]$ with $w_g = +0.1$. For this partial $\mathbf{g}\cdot\mathbf{b} = -1/3$ and $m = 1/8\ \mathbf{g}\cdot\mathbf{b}\times\mathbf{u} = -0.029$ and therefore it should not show any contrast[14]. However, it is clear that a relatively sharp black-white contrast is present due to the surface relaxation effect, which renders the invisibility criteria invalid.

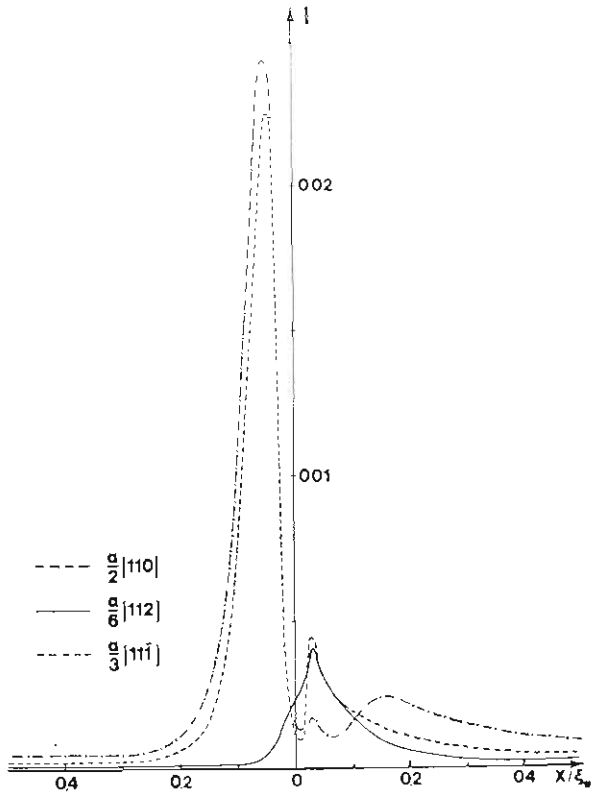

Fig. 7. Weak-beam image profiles as those in Fig. 6, except that now $g=[\bar{2}\,\bar{2}0]$.

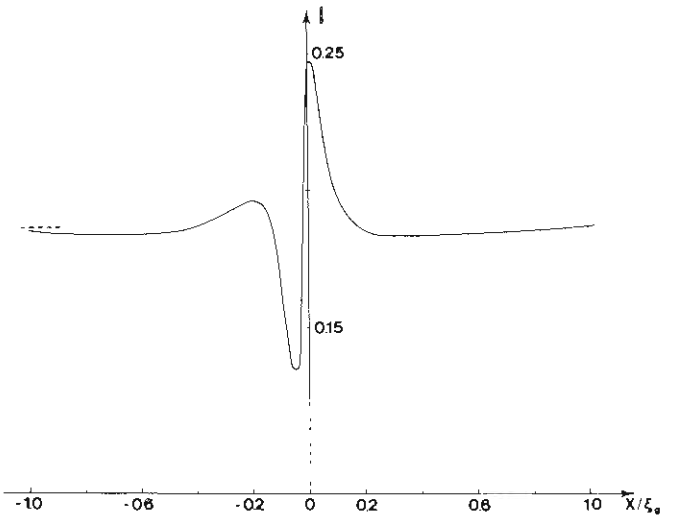

Fig. 8. Computed bright-field profile of a Schockley partial with $b=\frac{a}{6}[\bar{1}1\bar{2}]$, *lying at a depth of* $0.103\xi_g$ ($\xi_g = 243.3$ Å) *along [110] direction.*$g=[111]$ *with* $w_g = +0.1$

REFERENCES

1. P. B. Hirsch, A. Howie, R. B. Nicholson, D. W. Pashley and M. J. Whelan. «Electron microscopy of thin films», Butterworths, London (1967).
2. S. Amelinkx, «The direct observation of dislocations» Acad. Press, New York (1964).
3. S. Amelinkx, R. Gevers, G. Remaut and J. Van Landuyt, «Modern diffraction and Imaging Techniques in Material Science», North-Holland (1970).
4. A. K. Head, P. Humble, L. M. Clarebrough, A. J. Morton and C. T. Forwood, «Computed electron micrographs and defects identification», North-Holland (1973).
5. M. F. Ashby and L. M. Brown, Phil. Mag. 8, 1083 (1963).
6. J. Weertman and J. R. Weertman, «Elementary dislocation theory», MacMillan, New York (1966).
7. S. Timoshenko and J. N. Goodier, «Theory of elasticity», Mac Graw-Hill, (1951).
8. A. Kuske and G. Robertson, «Photoelastic stress analysis» John Wiley (1974).
9. A. K. Head, Proc. Phys. Soc. (London) 66 B, 793 (1953).
10. A. Howie and Z. S. Basinski, Phil Mag. 17, 1039 (1968).
11. C. J. Humphreys and P. B. Hirsch, Phil. Mag. 18, 115 (1968).
12. G. H. Smith and R. E. Burge, Acta Cryst. 15, 182 (1962).
13. D. J. H. Cockayne, I. L. F. Ray and M. J. Whelan, Phil. Mag. 20, 1265 (1969).
14. A. Howie and M. J. Whelan, Proc. R. Soc. London, A267, 206 (1962).
15. D. Cherns and M. J. Stowell, Thin Solid Films 29, 107 (1975).

APPENDIX A

```
      UZ=UZV+UZP
      UX=UXV+UXP
      IF(ML-3) 50, 26, 51
50    IF(BUDTW) 29, 26, 31
29    XM=-DEP*SNA/CNA
      GO TO 35
31    XM=DEP*SNA/CNA
      GO TO 34
51    IF(BUDTW) 27, 26, 33
27    XM=-DEP*CNA/SNA
      GO TO 34
33    XM=DEP*CNA/SNA
      GO TO 35
34    IF(XTEM) 36, 26, 26
36    IF(XM+XTEM) 26, 40, 40
40    IF((Z1/(XM+XTEM))-(DEP/XM)) 38, 38, 26
35    IF(XTEM) 26, 26, 37
37    IF (XM-XTEM) 26, 41, 41
41    IF ((Z1/(XM-XTEM))-(DEP/XM)) 32, 32, 26
32    R1(I1)=UX*XP1+UZ*W1-BU1
      R2(I1)=UX*XP2+UZ*W2-BU2
      R3(I1)=UX*XP3+UZ*W3-BU3
      GO TO 12
38    R1(I1)=UX*XP1+UZ*W1+BU1
      R2 I1)=UX*XP2+UZ*W2+BU2
      R3(I1)=UX*XP3+UZ*W3+BU3
      GO TO 12
26    R1(I1)=UX*XP1+UZ*W1
      R2(I1)=UX*XP2+UZ*W2
      R3(I1)=UX*XP3+UZ*W3
12    CONTINUE
```

ΠΕΡΙΛΗΨΗ

ΚΑΤΑΝΟΜΗ ΤΗΣ ΕΝΤΑΣΗΣ ΚΑΘΕΤΑ ΣΕ ΕΙΚΟΝΕΣ ΕΞΑΡΜΟΣΕΩΝ ΠΟΥ ΒΡΙΣΚΟΝΤΑΙ ΚΟΝΤΑ ΣΤΗΝ ΕΠΙΦΑΝΕΙΑ ΤΟΥ ΚΡΥΣΤΑΛΛΟΥ

Ὑπὸ

Ι. Γ. ΑΝΤΩΝΟΠΟΥΛΟΥ

Μὲ τὴ βοήθεια ἑνὸς προγράμματος κατασκευάστηκαν καμπύλες κατανομῆς τῆς ἔντασης κάθετα στὴ γραμμὴ τῆς ἐξάρμοσης. Τὸ πρόγραμμα παίρνει ὑπόψη του τὴν ἐπίδραση τῆς ἐλεύθερης ἐπιφάνειας στὶς μετατοπίσεις ποὺ προκαλεῖ μιὰ ἐξάρμοση σ' ἕνα πλέγμα, ὅπως ἐπίσης καὶ τὴν πιθανὴ δημιουργία σφάλματος ἐπιστοίβασης. Ἐξετάστηκαν πέντε πιθανὲς κατ' ἀκμὴ ἐξαρμόσεις ἀπὸ τὶς ὁποῖες τέσσερις ἦταν κλασματικὲς (2 Shockley καὶ 2 Frank) καὶ μία τέλεια. Αὐτὲς οἱ ἐξαρμόσεις ἔχουν διανύσματα Burgers στὸ ἴδιο ἐπίπεδο καὶ ἑπομένως τὸ κριτήριο $\mathbf{g} \cdot \mathbf{b} = 0$ δὲν μπορεῖ νὰ ἐφαρμοστεῖ μὲ ἐπιτυχία γιὰ τὸ διαχωρισμό τους. Τὰ ἀποτελέσματα τῆς ἐργασίας αὐτῆς ἔδειξαν ὅτι, κάτω ἀπὸ ὁρισμένες προϋποθέσεις, εἶναι δυνατὸς ὁ διαχωρισμὸς ἀνάμεσα στὰ τρία εἴδη ἐξαρμόσεων (τῆς Shockley, τῆς Frank καὶ τῆς τέλειας).